ehp ENVIRONMENTAL HEALTH PERSPECTIVES
http://www.ehponline.org

Characterizing the Peroxisome Proliferator–Activated Receptor (PPARγ) Ligand Binding Potential of Several Major Flame Retardants, Their Metabolites, and Chemical Mixtures in House Dust

M. Fang, T.F. Webster, P.L. Ferguson, and H.M. Stapleton

http://dx.doi.org/10.1289/ehp.1408522

Received: 7 April 2014
Accepted: 9 October 2014
Advance Publication: 14 October 2014

Characterizing the Peroxisome Proliferator–Activated Receptor (PPARγ) Ligand Binding Potential of Several Major Flame Retardants, Their Metabolites, and Chemical Mixtures in House Dust

M. Fang,[1] T.F. Webster,[2] P.L. Ferguson,[1] and H.M. Stapleton[1]

[1]Nicholas School of the Environment, Duke University, Durham, North Carolina, USA;

[2]Department of Environmental Health, Boston University School of Public Health, Boston, Massachusetts, USA

Address correspondence to Heather Stapleton, Nicholas School of the Environment, Duke University, LSRC, Box 90328, Durham, NC. Telephone: 919-613-8717. E-mail: heather.stapleton@duke.edu

Short running head: Flame retardants and metabolites bind to human PPARγ

Acknowledgments: The author would like to thank Katherine Stencel from the Nicholas School of the Environment, Duke University for her assistance with the use of the SpectraMax M5 plate reader. This study was funded by grants from the National Institute of Environmental Health Sciences (R01ESO16099, R01 ES015829, and P42ES00738) and Boston University School of Public Health pilot funding.

Competing financial interests: The authors declare no competing financial interests.

Abstract

Background: Accumulating evidence has shown that some environmental contaminants can alter adipogenesis and act as obesogens. Many of these contaminants act via the activation of the peroxisome proliferator activated receptor γ (PPARγ) nuclear receptor.

Objectives: Our goal was to determine the PPARγ ligand binding potency of several major flame retardants, including polybrominated diphenyl ethers (PBDEs), halogenated phenols and bisphenols, and their metabolites. Ligand binding activity of indoor dust and its bioactivated extracts were also investigated.

Methods: A commercially available fluorescence polarization ligand binding assay (PolarScreen^{TM} PPARγ-competitor assay kit, Invitrogen) was used to investigate the binding potency of flame retardants and dust extracts to human PPARγ LBD. Rosiglitazone was used as a positive control.

Results: Most of the tested compounds exhibited dose-dependent binding to PPARγ. Mono(2-ethylhexyl) tetrabromophthalate (TB-MEHP), halogenated bisphenol/phenols, and hydroxylated PBDEs were found to be potent PPARγ ligands. The most potent compound was 3-OH-BDE47, with an IC_{50} of 0.24 μM. The extent of halogenation and the position of the hydroxyl group strongly affected binding. In the dust samples, 21 of the 24 samples tested showed significant binding potency at a concentration of 3 mg dust equivalent (DEQ)/mL. A 3–16% increase in PPARγ binding potency was observed following bioactivation of the dust using rat hepatic S9 fractions.

Conclusion: Our results suggest that several flame retardants are potential PPARγ ligands, and that metabolism may lead to increased binding affinity. The PPARγ binding activity of house

dust extracts at levels comparable to human exposure warrants further studies into agonistic or antagonistic activities and their potential health effects.

Introduction

According to a report from the Center for Disease Control and Prevention (CDC), 17% of children between 2 and 19 years of age are obese in the US, and the health care costs associated with obesity were estimated to be more than $140 billion in the US in 2008 (Ogden et al. 2012). While genetics, diet, and exercise all contribute to obesity, recent studies have shown that prenatal exposures to "environmental obesogens" including bisphenol A, phthalates, organotins and perflourinated compounds may increase the risk of obesity in children (Janesick and Blumberg 2011). Several studies found significant associations between urinary metabolites of phthalates and obesity (Wang et al. 2013). High levels of several persistent organic pollutants (e.g., DDE, hexachlorobenzene, and polybrominated diphenyl-ethers (PBDEs)) have also been found to be associated with obesity in humans (Tang-Peronard et al. 2011).

Current research suggests that several of the obesogenic compounds act via a mechanism involving activation of peroxisome proliferator-activated nuclear receptors (PPARs) during perinatal development (Janesick and Blumberg 2011). PPARs are master transcriptional regulators controlling intracellular lipid flux and adipocyte proliferation and differentiation. Heterodimerized with the retinoid X receptor, PPARs serve as metabolic ligand sensors for a variety of hormones, dietary fatty acids, and their metabolites (Grün and Blumberg 2009). Chemicals that specifically activate PPARγ and upregulate expression may promote the development of obesity. Studies investigating the crystal structure of PPARγ with thiazolidinedione drugs have found that it exhibits flexible plasticity in the ligand-binding domain (PPARγ LBD), which allows it to accommodate a wide variety of ligands (Nolte et al. 1998). The endogenous ligands of PPARγ include polyunsaturated fatty acids, prostanoids, and oxidized fatty acids. Several anti-diabetic drugs of the thiazolidinedione class such as

rosiglitazone target PPARγ (Lu and Cheng 2010) and weight gain is often a side effect (Ness-Abramof and Apovian 2005). Environmental contaminants including tributyltin (TBT), triphenyltin (TPT), and mono(2-ethylhexyl) phthalate bis(2-ethylhexyl) (MEHP) (a metabolite of the phthalate DEHP), have been shown to upregulate and stimulate several PPARs (Feige et al. 2007).

Flame retardants (FRs) are a class of compounds that have been used in large volumes over the past few decades to reduce the flammability of textiles, polymers and resins. Accumulating evidence has suggested that FRs might represent an important class of compounds that could bind to PPARγ and disrupt signaling. A recent study found that 2,2,6,6′ -tetrabromo bisphenol (TBBPA) and 3,3',5,5'-tetrachlorobisphenol A (TCBPA), were agonists of PPARγ (Riu et al. 2011). In our recent studies, Firemaster® 550 (FM550), a FR replacement for pentabromodiphenyl ethers (Penta-BDEs), activated PPARγ and initiated adipocyte differentiation *in vitro* (Pillai et al. 2014), which may explain why perinatal exposure to FM550 in rats lead to obesity and glucose sensitivity (Patisaul et al. 2013). Therefore, further investigation of PPARγ-targeted disruption by FRs is warranted.

Several organophosophate compounds are also structurally similar to PPARγ exogenous agonists. For example, tributylphosphate (TBuP) and tris(2-butoxyethyl) phosphate (TBEP) are structurally similar to TBT. The PPARγ ligand triphenyl phosphate (TPP) and its antioxidant analogue triphenylphosphite (TPPi) resemble TPT. Many of the PBDE metabolites (i.e., hydroxylated PBDEs and halogenated phenols) are structurally similar to TBBPA, which was shown to be a PPARγ ligand. Therefore, it would be of great interest to investigate whether these structurally similar compounds could also act on PPARγ.

Indoor dust is a primary sink for additive chemicals applied to consumer products, and many of the reported environmental obesogens are found abundantly in house dust. For example, DEHP was detected in all dust samples analyzed with a geometric mean concentration of 340,000 ng/g (Rudel et al. 2003), and organotins are also commonly detected (Kannan et al. 2010). Three of the four chemicals in FM550 were widely detected in house dust samples in the US (Dodson et al. 2012; Stapleton et al. 2014). Young children in the US spend a majority of their time (>95%) indoors where they are chronically exposed to FRs due to increased hand to mouth activity (U.S. EPA 2009). Therefore, it is important to investigate the PPARγ binding potency of environmentally relevant house dust samples.

Little attention has also been given to the effect of bioactivation on PPARγ disruption. Several studies have revealed that metabolites can be more potent endocrine disruptors than the parent compounds. For example, the metabolite MEHP exhibited much stronger PPARγ binding potency than its parent compound, DEHP (Feige et al. 2007). Tetrabromo mono(2-ethylhexyl)phthalate (TBMEHP), a metabolite of bis(2-ethylhexyl) tetrabromophthalate (TBPH), has also been reported to be an agonist for PPARs in mouse NIH 3T3 L1 preadipocyte cells, whereas TBPH was not (Springer et al. 2012). The chemicals present in ingested house dust are absorbed into the digestive system and can be metabolized to chemicals with more polar functional groups. Therefore, it is important to determine whether PPARγ binding potency of contaminants changes with metabolism.

The primary goals of this study were to: 1) characterize the binding potency of several major FRs such as PBDEs (and their metabolites) using a human protein–ligand binding assay; 2) test the PPARγ binding activity of indoor dust extracts; and 3) examine the effect of *in vitro* bioactivation on the PPARγ binding potency of dust extracts.

Materials and Methods

Chemicals

The tested compounds included FM550 (and their metabolites), several PBDE congeners (and their metabolites), halogenated phenols and bisphenols. All the abbreviation was shown in Supplemental Material, Abbreviation. Rosiglitazone and MEHP were used as positive controls. The chemical structures of all the tested compounds are shown in Supplemental Material, Figure S1. 2,2',4,4'-tetrabromodiphenyl ether (BDE-47) and 2,2',4,4',5-pentabromodiphenyl ether (BDE-99), their metabolites [i.e., 3-OH-BDE-47, 5-OH-BDE-47, 6-OH-BDE-47, 5'-OH-BDE-99, and 6'-OH-BDE-99], and TBBPA (98%) were purchased from AccuStandard (New Haven, CT). 2,4,6-tribromophenol (2,4,6-TBP, 99%), 2,4,6-triiodophenol (2,4,6-TIP, 97%), 2,4,6-trifluorophenol (2,4,6-TFP, 99%), 2,4,6,-trichlorophenol (2,4,6-TCP, 98%), TPP (99%), diphenyl phosphate (DPP, 99%), rosiglitazone (98%), triclosan (> 97%), TBT (96%), TBEP (94%), TPPi (97%), DL-dithiothreitol (DTT, >99%), β-nicotinamide adenine dinucleotide 2′-phosphate reduced tetrasodium salt hydrate (β-NADPH, >93%), magnesium chloride (hexa-hydrates, >99%), and dextran (Leuconostoc spp., MW: 6,000 to 10,000) were purchased from Sigma-Aldrich (St Louis, MO). TPT (95%) was purchased from ACROS Organics (NJ, USA). TCBPA (98%) was purchased from TCI America (Portland, OR). Tetrabromobenzoic acid (TBBA; estimated > 98% purity by H1-NMR), was synthesized by the Duke Small Molecule Synthesis Facility. TBMEHP was a gift from Dr. Kim Boekelhide's group at Brown University. MEHP (98%) was purchased from Wako Pure Chemical Industrials, Ltd (Osaka, Japan). A commercial standard of FM 550 was supplied by Great Lakes Chemical (West Lafayette, IN), a company owned by Chemtura (Philadelphia, PA). ITP commercial mixture was purchased from one manufacturer in China. All solvents and other materials were of HPLC grade.

Chemical analysis

To investigate the elution profile of chemicals in the gel permeation chromatography (see Supplemental Material, Operation of Gel Permeation Chromatography), DEHP, MEHP, TBBPA, TBBA and other tested compounds were quantitatively analyzed by either liquid chromatography tandem mass spectrometry (Agilent 6410 Triple Quad LCMS) or gas chromatography coupled with mass spectrometry detector (GC-MSD). The details of the parameter used in this study were described in Supplemental Material, Table S1.

PPARγ competitive binding assay

A detailed description of the PPARγ binding assay is shown in Supplemental Material, PPARγ Competitive Binding Assay. Briefly, a commercially available high-throughput ligand binding assay (PolarScreen^{TM} PPARγ-competitor assay kit, Invitrogen) was used to investigate the binding potency of tested compounds to PPARγ LBD. The kit uses the human-derived recombinant PPARγ-LBD tagged with a N-terminal GST-tag and a selective fluorescent PPARγ ligand (PPARγ Green). A SpectraMax M5 plate reader was used in fluorescence polarization (FP) mode with 485 nm excitation and 535nm emission wavelength. To measure ligand binding, we quantified polarization (mP) of the bound protein using the following equation:

$$mP = 10^3*(I_p-I_s)/(I_p+I_s) \quad [1]$$

where I_p and I_s are the fluorescence intensity of emissions that are parallel (P) and perpendicular (S) to the excitation light; respectively (Rossi and Taylor 2011).

Dust sample dosing

Extracts of indoor dust samples (n=23) collected from our previous studies and a dust Standard Reference Material (SRM 2585, National Institute of Standards and Technology (NIST),

Gaithersburg, MD) were tested for ligand binding potential. The indoor dust samples were investigator-collected from the main living areas of homes for Group A (Stapleton et al. 2012) and D (Stapleton et al. 2014). Dust samples in Group B were collected from gymnastics studios (Carignan et al. 2013b). Dust samples in Group C were investigator collected from office environments (Watkins et al. 2013), and Group E were participant-collected dust samples from the main living area as reported in Hoffman et al. (2014). All dust samples were extracted with acetone:hexane (1:1, v/v) using sonication, and then concentrated, filtered and reconstituted in dimethyl sulfoxide (DMSO). Fluorescence background (FB) from the dust matrix was initially observed in the dust extracts (observed by spiking the incubation buffer solution with the extract but without PPARγ LBD and PPARγ Green). Therefore, the dust extracts were cleaned and diluted prior to measuring the PPARγ ligand binding activity. As shown in Supplemental Material, Figure S2 (a), a FB dose-response of SRM 2585 was observed and dilution greatly reduced the FB from the dust matrix. In this study, gel permeation chromatography (GPC, Environgel GPC system (Waters, Milford, CA, USA)) cleanup, which can partially remove large molecular weight (MW) compounds containing fluorophores, was used to clean the extracts (See Supplemental Material, Material Operation of Gel Permeation Chromatography and Table S2). To minimize FB, further dilution was performed until no obvious FB (i.e., < 5% intensity of the complex consisting of 1.25nM PPAR-Green and 38nM PPARγ LBD) was observed. Following GPC cleanup and dilution, a single concentration of 3 mg dust equivalent quantity (DEQ)/mL PPARγ assay medium was prepared to qualitatively investigate the relative PPARγ binding potency of the dust samples and the full dose-response of one potent dust extract was investigated. To quantitatively estimate the effect of FB on the polarization values (mP), we spiked the positive control (rosiglitazone, 12.5μM) into several different dose levels of a

SRM2585 extract previously cleaned by GPC to measure the ligand binding activity relative to the pure standard.

Bioactivation of dust samples

The influence of biotransformation on ligand binding activity was assessed by incubating dust extracts in pooled liver S9 fractions prepared from Sprague Dawley rats (Gibco, Grand Island, NY). Bioactivation was assessed in 7 of the 23 dust samples (one dust sample was tested in triplicate while the others were tested once due to dust mass limitations) and in SRM 2585 (n=3). The 7 dust samples were from Group A (Samples 5,7,8), B (Samples 9,10) and C (Samples 11,12). The influence of biotransformation was also investigated using pure chemical standards. DEHP (100μM) and a mixture (MIX) containing 1μM each of FM550, isopropylated triaryl phosphate (ITP), BDE47, BDE99, and DEHP were evaluated for binding activity before and after bioactivation. A detailed description of the method is shown in Supplemental Material, Bioactivation of Dust Samples and S3. Briefly, dust samples were bioactivated by incubation with an S9 fraction (1 mg protein/mL), extracted, and cleaned by dextran-assisted liquid-liquid extraction and phenolic extraction. An additional sample of each dust extract was incubated with inactive S9 fraction (by adding 150 μL of ice-cold 6 M HCl before incubation) to serve as a control. To test the efficacy of metabolism, MEHP, which is a metabolite of DEHP in house dust, was used as a marker compound to optimize the incubation method (See Supplemental Material, Figure S4). To compare the bioactivation difference between rodents with human, a pooled human liver S9 (CellzDirect, Durham, NC) was also used to bioactivate SRM2585.

Data analysis

IC_{50} values and dissociation constants were calculated to compare the binding potency. In this competitor study, the dose-response curve was depicted as ligand-binding, three parameter sigmoidal dose-response model in the ‘‘Regression Wizard’’ in SigmaPlot 12.0 (Systat Software Inc., Chicago, IL):

$$y = min + (max - min)/(1 + 10^{(\log IC_{50} - x)}) \quad [2]$$

where y is the measured polarization value (mP); x is the log of the compound concentration; *max* is the mP of the DMSO control or the maximum mP of the tested compounds; *min* is the the basal mP when reference agonists completely inhibit the binding between PPARγ LBD and PPAR-Green. Since *min* was not zero and varied between batches, high doses of rosiglitazone (10 μM) were run alongside each batch to roughly calculate the $min_{norminal}$. The dissociation constants were calculated according to the following equation (Lin et al. 1999):

$$IC_{50}/[\text{PPARγ Green}] = K_{d,ligand}/K_{d,probe}, \quad [3]$$

where $K_{d,probe}$ is the dissociation constant calculated from titration of 1.25 nM PPARγ Green with added PPARγ-LBD concentration.

Statistical analyses

All statistical analyses were conducted using SigmaPlot 12.0 (Systat Software Inc.), testing hypotheses at $\alpha = 0.05$, and all tests were two-tailed. When comparing the binding potencies of the dust extracts, all the FP values of the dust samples were normalized to the procedural blank. Then a one way *ANOVA* was conducted and Newman-Keuls *post-hoc* test was used to identify which dust extracts were significantly different from the procedural control. When comparing

the PPARγ binding activity before and after metabolism, all the data were normalized to the mP of the S9 control and student *t*-test was used to test the difference between active S9 and inactive S9 for the dust samples with triplicate incubations. For the bioactivated dust (n = 6) with single measurements, paired *t*-test was conducted. Quality control is described in Supplemental Material, Quality Assurance/Quality Control.

Results

Performance of the FP assay

We used rosiglitazone as a positive control in the ligand binding assay. As shown in Table 1, the IC_{50} of rosiglitazone was 0.23 μM. The FP range was more than 120 mP, indicating a good dynamic range for the dose-response. A PPARγ-LBD titration curve was also investigated by varying the protein concentration in 1.25 nM PPAR-Green (See Supplemental Material, Figure S5). In this study we used 38 nM of the PPARγ-LBD, which was in the linear range of the titration curve, providing a calculated K_d of 20 nM. A "U" shaped dose-response curve was observed for some tested compounds, which was probably due to limited solubility and precipitation of the compounds. Under such circumstances, the FP values of the concentration on the right side of the "U" shape were discarded for data analysis and partial dose-response curves were analyzed. The primary challenge of this assay was the fluorescence interference from the dust matrix in the extracts. As shown in Supplemental Material, Figure S2 (a), GPC cleanup can reduce the FB significantly, which suggests that macromolecules might be resulting in the observed interference. After further dilution, a dose of 3 mg DEQ/mL was used for the dust samples. In the matrix-spiked rosiglitazone test, the binding activity of rosiglitazone was completely masked at high matrix background (12.5 mg DEQ/mL) (See Supplemental Material, Figure S6). The FB of house dust increased the fluorescence intensity of emission parallel (P) to

the excitation plane more than that perpendicular (S) to the excitation plane, which resulted in the increased mP. It is impossible to completely eliminate the background interference, and exhaustive cleanup increases the possibility of analyte loss. We estimate that at the dosing concentration used in this study (3 mg DEQ/mL), the binding potency of house dust might actually be underestimated by 5-10% due to the fluorescence interference from the dust matrix. This estimate is based on the difference between the fluorescent signals in dust extracts spiked with and without rosiglitazone (see Figure S6). Overall, we conclude that the FP assay was appropriate and efficient to evaluate the binding potency of the tested compounds and dust extracts. The dose-response curves of the tested compounds were shown in Supplemental Material, Figure S7, and the calculated IC_{50} together with K_d was listed in Table 1.

FM550 metabolites

Using this assay, we recently demonstrated that while the organophosphate components in FM550 did bind to PPARγ, the brominated components, TBB and TBPH, did not (Pillai et al. 2014). We also investigated the binding affinities of potential metabolites of the individual FM550 components [See Figure 1 (a)]. We found that the metabolites of TBB and TBPH, TBBA and TBMEHP (Roberts et al. 2012), respectively, can bind PPARγ effectively. As shown in Table 1, TBBA was found to be a moderately potent ligand of PPARγ with an IC_{50} of 42 μM. The binding of TBMEHP was particularly potent with an IC_{50} of 0.64 μM, which was much lower than the well-known PPARγ agonist MEHP (3.8 μM) and comparable to PPARγ binding pharmaceutical compound rosiglitazone (IC_{50}: 0.23 μM). The metabolite of TPP (IC_{50}: 40 μM), DPP (IC_{50}: 627 μM), was one order of magnitude less potent than its parent compound.

Halogenated phenols/bisphenols

Phenols and biphenol compounds with different degrees of halogenations were also tested for binding with PPARγ. A dose-response relationship was observed for all the tested phenols except 2,4,6-trifluorophenol (2,4,6-TFP). Potency increased with size of the halogen in order of F<Cl (IC_{50}:100 μM)<Br (IC_{50}: 36.3 μM)<I (IC_{50}: 1.84 μM) [see Figure 1(b) and Table 1]. A significant FB was observed for TIP at concentrations over 10μM. A similar trend in binding with halogenation was observed for TBBPA (IC_{50}:1.49 μM) and TCBPA (IC_{50}: 5.18μM), which are known PPARγ ligands; however, BPA did not exhibit any binding. Triclosan, which is largely applied in personal care products, also exhibited PPARγ binding with an IC_{50} of 12.5μM.

BDE and BDE metabolites

The binding activity of BDEs was very poor. The calculated IC_{50} for BDE47 was >12μM, and no binding was observed for BDE99 at any dose tested. However, some of the OH-BDEs were found to be very potent ligands of PPARγ (See Table 1). The BDE47 metabolite 3-OH-BDE47 (IC_{50}: 0.24μM) showed a similar binding capacity with the positive control rosiglitazone, followed by 5-OH-BDE47 with a calculated IC_{50} of 3.09μM. In contrast 6-OH-BDE47 and 6-OH-BDE99 were not active ligands for PPAR γ . The calculated IC_{50} for 5-OH-BDE 99 was 30 μM.

Organophosphate/phosphite analogues of organotin

As shown in Table 1, TBuP, TBEP, TPPi, and TPP were found to bind to the *PPARγ LBD*; however, the IC_{50} varied greatly between the compounds. TBuP (IC_{50}: 137μM) and TBEP (IC_{50}: 103μM) were two orders of magnitude less potent than TBT (IC_{50}: 0.3μM). However, we also observed that TBuP could completely inhibit the binding between the probe and the PPARγ LBD

at the high concentration (2,500μM, see Supplemental Material, Figure S7). TPPi was much less potent at binding than TPP (IC_{50}: 40 μM) and TPT (IC_{50}: 1.72μM) with an IC_{50} >1,250μM.

Binding activity of dust samples

Significant PPARγ binding activity of the dust samples at a concentration of 3 mg DEQ/mL was observed for 21 of the 24 dust samples tested (see Figure 2). No significant binding was observed for SRM2585. High variability was observed between the dust samples. Ten of the dust extracts competitively inhibited the binding between the PPARγ LBD and PPARγ Green by more than 40% of the control. The binding potency of those dust extracts was only slightly lower than the positive control (12.5μM of rosiglitazone), which could completely inhibit the binding between the PPARγ and Green probe. Dust (DS) 6, which demonstrated a high binding potency, was selected to quantitatively evaluate the binding potency, and a clear dose-response relationship was observed [see Supplemental Material, Figure S8 (a)]. The calculated IC_{50} of DS6 was approximately 0.37 mg DEQ/mL. We also observed differences in binding potency among dust extracts from different sources. For example, the dust extracts from Groups A and D, which were collected from main living areas in homes, showed a higher binding affinity with PPARγ than other groups (see Figure 2). In contrast, the Group B samples collected from gymnastic studios did not show any obvious binding.

Bioactivated dust samples

No difference in ligand activity was observed between the extracts of active and inactive S9 fractions alone (i.e., S9 control, see Figure 3). A slight increase in the potency of PPARγ binding was observed after bioactivation of 100μM DEHP (n=3), and the bioactivated MIX (n=3), which was about a ~5% increase in binding (i.e., ~10 mP). Bioactivated SRM2585 using rat liver S9

fraction was significantly more potent with an approximately 16% (i.e., 40 mP) increase in inhibition. A similar increase (~18%) was observed in SRM2585 incubated with the human liver S9 fraction, suggesting similar bioactivation effects on PPARγ binding. In DS5, a significant increase (~13%) in the binding was also found after bioactivation. A slight increase (3–10%) was also observed in other incubated dust samples. A paired *t*-test including all the dust samples with single incubations revealed that bioactivated dust samples showed significantly stronger binding potency with PPARγ than dust samples incubated with inactive S9 fraction ($p < 0.01$). To quantitatively observe the change with different doses, a dose-response analysis was conducted to investigate the binding potency of the MIX, bioactivated MIX, and SRM2585. A partial dose-response curve was observed because the dust matrix or S9 co-extracts interfered with polarization at high doses [see Supplemental Material, Figure S2 (c) and (d)]. As shown in Supplemental Material, Figure S8 (b), higher inhibition potency was observed for the bioactivated MIX in the dynamic range of the dose-response curve. Bioactivated SRM2585 also showed a dose response curve [see Supplemental Material, Figure S8 (c)], although no inhibition was observed for the nonactivated extract [see Figure 2 (a)]. Thus our data indicate that PPARγ binding potency of dust samples increases after metabolism.

Discussion

PPARγ is a master nuclear receptor that regulates lipid metabolism, cell proliferation signal transduction, apoptosis, and differentiation. Until now, few environmental contaminants have been shown to significantly bind and activate PPARγ signaling. This study was designed to test the PPARγ binding potency of several major FRs including FM550, and PBDEs, and their metabolites using a ligand-binding competitor assay. Furthermore, the PPARγ binding of SVOCs structurally similar to known PPARγ agonists, such as organotins and halogenated bisphenols,

was examined. The binding potency of house dust samples and their bioactivated extracts was also examined. To our knowledge, very few studies have been conducted to investigate PPARγ activity in environmentally relevant dust samples. However, it should be noted that no definitive conclusions can be drawn from this PPARγ binding data as to whether these samples would lead to transactivation of PPARγ.

Data presented here is consistent with data reported in previous studies based on a luciferase gene reporter cell line assay. The *in vitro* binding of FM550 and its components were consistent with the Cos-7 luciferase reporter assay, indicating that TPP was the major contributor to the PPARγ binding in the commercial mixtures (Pillai et al. 2014). The relative potency of TBBPA and TCBPA tested in this study was also similar to the results of the HGELN-GAL-PPAR assay reported by (Riu et al. 2011). Therefore, our study showed that this direct protein–ligand binding competitor assay could be used as an effective alternative method in the early screening of PPARγ ligands.

In this study, we found that several of the tested chemicals or their metabolites can competitively bind with the PPARγ LBD. The calculated IC_{50} values and K_d of the tested compounds with the PPARγ-LBD varied considerably. Most of the previously reported potential PPARγ ligands (e.g., TBBPA, TCBPA, TB-MEHP, TBT, and TPT) were confirmed in this study using a different bioassay. To the best of our knowledge, many of the compounds tested here, including halogenated phenols, several hydroxylated metabolites of PBDEs and FM550, TBuP, TBEP and TPPi were shown for the first time to have PPARγ binding activity. Although some of the tested compounds (e.g., TBEP and TBuP) showed weaker PPARγ binding potency, these compounds may yet be of great concern because of their ubiquitous detection in indoor environments, with levels up to μg-mg/g (Van den Eede et al. 2011).

Our study also revealed that metabolites of many FRs can be more potent than their parent compounds. PBDEs are a group of FRs that has increased public health concerns for decades due to potential disruption of thyroid hormone regulation and neurodevelopment (Noyes et al. 2011). BDE-47 and -99, which were predominant components of the banned PentaBDE commercial mixture that are still widely detected in the environment, did not show strong binding potency to PPARγ. However, OH-BDEs, which are formed through cytochrome P450-mediated oxidative metabolism of BDEs, were found to be potent PPARγ ligands in the present study. The metabolite 3-OH-BDE-47 exhibited a comparable binding potency to the drug rosigilitazone. 5-HO-BDE-47, which is one of the most abundant metabolites of BDE-47 (Qiu et al. 2007), also showed a very strong binding potency. Due to their high potency, further studies on the role of OH-BDEs in PPARγ signaling disruption should be investigated. Although the other two major components of FM550, TBB and TBPH, did not show any binding activity, their metabolites (TBMEHP and TBBA) can be potent ligands of PPARγ. While TBMEHP is not readily metabolized from its parent TBPH by enzymes in human hepatic S9 fractions or microsomes in our previous *in-vitro* studies (Roberts et al. 2012), the other major metabolites (i.e., DPP and TBBA) have been frequently identified in human urine samples (Cooper et al. 2011; Hoffman et al. 2014; Meeker et al. 2013). To date, little toxicological information has been reported for TBBA, and further studies on its potential to disrupt PPARγ should be investigated.

Our results also highlight several characteristics that may increase binding potency to PPARγ. First, halogenation, especially bromination, increases the potency of PPARγ binding, which was confirmed by the specific binding activities of halogenated phenols and bisphenols. The flame retardant 2,4,6-TBP showed a similar binding potency with TPP. Our structure-activity relationship experiments showed that the inhibition potency generally increased with increasing

halogen molecular weight (i.e., I > Br > Cl > F), which suggests that non-specific hydrophobic interactions (i.e., Van der Waals force) with the PPARγ binding pocket favor binding. These findings are consistent with studies investigating T4-TTR binding affinity and deiodination activity inhibition (Meerts et al. 2000). A similar trend was also observed for TCBPA and TBBPA, which was consistent with a previous study suggesting that bulkier compounds bind more strongly with PPARγ (Riu et al. 2011). The IC_{50} of TB-MEHP was one order of magnitude lower than the IC_{50} of MEHP, which suggests that halogenation supports binding. All these findings indicate that the large ligand binding pocket of PPARγ can readily accommodate the addition of bulky bromine or chlorine. Therefore, disruption of PPARγ signaling may be a major concern for FRs because a large number of FRs are halogenated. Second, we also found that the number of halogens and the position of the hydroxyl group affect PPARγ binding. In this study, a dose-response relationship for BDE-47 was observed, but no binding was observed with BDE-99. Suzuki et al. (2013) also observed a dose- response relationship between PPARγ2 and BDE-47 with a 5% induction concentration of 10μM using a human osteosarcoma (U2OS) cell-based reporter assay (Suzuki et al. 2013), but no activity was observed for other BDEs. The variable IC_{50} values of BDEs and OH-BDEs suggest that the OH-BDEs with a *meta* hydroxyl group exhibited stronger PPARγ binding potency than OH-BDEs with an *ortho* substituted hydroxyl group. Among all the OH-BDEs tested, 3-OH-BDE-47 showed the most similar structure to the known PPARγ agonist TBBPA, with a *meta*-substituted hydroxyl group and two adjacent bromine atoms. Lastly, we observed that the PPARγ binding potency differed greatly for chemicals with similar structures. Organophosphates were more potent than the organophosphites, but both were much less potent than the organotins, which suggests that some other chemical feature, perhaps the electron density of the tin atom, might play an important role

in the binding. Alternatively, this also may be related to the relative solubilities of the compounds.

To date, few toxicological studies have investigated potential health effects from environmentally relevant house dust samples, which are more insightful than exposures of pure chemicals with regards to human exposure. Because many SVOCs bind to dust in the indoor environment, dust samples were tested for the PPARγ binding potency in this study. Binding activity was observed in most of the dust samples (21 out of 24 dust samples) and differences were observed between groups of dust extracts. To date, no characterization of the chemical composition in the dust samples from different sources has been conducted. In our previous study, FRs especially PBDEs in the dust from gymnasium (Carignan et al. 2013a), were found at least one order of magnitude higher concentrations than levels in residential dust, suggesting those FRs might not be the primary contributor to the PPARγ binding. However, the small sample size and heterogeneity of the house dust samples prevent any solid conclusions from being made. Also, the binding potency of the house dust in this study might be underestimated due to FP interference from the dust matrix. Young children spend most of their time indoors and are exposed to house dust via frequent hand-to-mouth behavior. Therefore, tests on dust samples are needed to determine the public health concerns for exposures to contaminant mixtures present in dust. The USEPA estimates that children ingest between 50–100 mg/dust day (U.S. EPA 2009) . In one of the most potent dust samples, an IC_{50} of 0.37 mg DEQ/mL was observed. Therefore, our data suggest that environmentally relevant dust exposures might interact with PPARγ *in vivo*.

We also investigated the bioactivation of dust samples to increase understanding of the potential activity *in vivo* following metabolism. Stronger binding potency was observed in the bioactivated

dust samples compared with the raw dust extracts. Bioactivation could transform the hydrophobic chemicals into more polar metabolites by adding polar groups such as –OH and –COOH, which might increase the binding interaction with the LBD through hydrogen bonds. It might be possible that several compounds such as TBB, TBPH, PBDEs, and DEHP in dust could be metabolized to PPARγ active ligands after incubation, which was supported by the increased binding potency of the prepared MIX containing these chemicals. While the effect of bioactivation was only on the order of less than ~20%, it is possible that *in vivo* metabolism would lead to higher binding activity. Chemicals in the human body would have a half-life that is longer than our two-hour incubation, and would lead to longer contact time with xenobiotic metabolizing systems in the body. Therefore, bioactivation should be considered when evaluating potency of environmental chemicals and potential human health risks.

Conclusion

In conclusion, this study showed that many of the tested compounds or metabolites are potential PPARγ ligands. Significant binding activity of environmentally relevant dust samples was also observed with high frequency. We also observed that bioactivation could increase the binding potency of chemical mixtures in the ingested dust. Further work is needed to determine which components in the dust samples are acting as ligands. A limitation of this study is that ligand binding does not necessarily indicate agonism of the receptor, leading to transcriptional events. Ligands can be agonists (full or partial) or competitive antagonists. To confirm the health effects of the identified PPARγ ligands, further studies using cell-based reporter assays that can distinguish between agonism and antagonism should be conducted.

References

Carignan CC, Heiger-Bernays W, McClean MD, Roberts SC, Stapleton HM, Sjodin A, et al. 2013a. Flame Retardant Exposure among Collegiate United States Gymnasts. Environ Sci Technol 47(23): 13848-13856.

Carignan CC, McClean MD, Cooper EM, Watkins DJ, Fraser AJ, Heiger-Bernays W, et al. 2013b. Predictors of tris(1,3-dichloro-2-propyl) phosphate metabolite in the urine of office workers. Environ Int 55: 56-61.

Cooper EM, Covaci A, van Nuijs ALN, Webster TF, Stapleton HM. 2011. Analysis of the flame retardant metabolites bis(1,3-dichloro-2-propyl) phosphate (BDCPP) and diphenyl phosphate (DPP) in urine using liquid chromatography-tandem mass spectrometry. Anal Bioanal Chem 401(7): 2123-2132.

Dodson RE, Perovich LJ, Covaci A, Van den Eede N, Ionas AC, Dirtu AC, et al. 2012. After the PBDE Phase-Out: A Broad Suite of Flame Retardants in Repeat House Dust Samples from California. Environ Sci Technol 46(24): 13056-13066.

Feige JN, Gelman L, Rossi D, Zoete V, Métivier R, Tudor C, et al. 2007. The endocrine disruptor monoethyl-hexyl-phthalate is a selective peroxisome proliferator-activated receptor gamma modulator that promotes adipogenesis. J Biol Chem 282(26): 19152-19166.

Grün F, Blumberg B. 2009. Endocrine disrupters as obesogens. Mol Cell Endocrinol 304(1-2): 19-29.

Hoffman K, Fang M, Horman B, Patisaul HB, Garantziotis S, Birnbaum LS, et al. 2014. Urinary Tetrabromobenzoic Acid (TBBA) as a Biomarker of Exposure to the Flame Retardant Mixture Firemaster(R) 550. Environ Health Perspect 122(9): 963-969.

Janesick A, Blumberg B. 2011. Minireview: PPARgamma as the target of obesogens. J Steroid Biochem Mol Biol 127(1-2): 4-8.

Kannan K, Takahashi S, Fujiwara N, Mizukawa H, Tanabe S. 2010. Organotin compounds, including butyltins and octyltins, in house dust from Albany, New York, USA. Archives of environmental contamination and toxicology 58(4): 901-907.

Lin Q, Ruuska SE, Shaw NS, Dong D, Noy N. 1999. Ligand selectivity of the peroxisome proliferator-activated receptor alpha. Biochemistry 38(1): 185-190.

Lu CX, Cheng SY. 2010. Thyroid hormone receptors regulate adipogenesis and carcinogenesis via crosstalk signaling with peroxisome proliferator-activated receptors. J Mol Endocrinol 44(3): 143-154.

Meeker JD, Cooper EM, Stapleton HM, Hauser R. 2013. Urinary Metabolites of Organophosphate Flame Retardants: Temporal Variability and Correlations with House Dust Concentrations. Environ Health Persp 121(5): 580-585.

Meerts IATM, van Zanden JJ, Luijks EAC, van Leeuwen-Bol I, Marsh G, Jakobsson E, et al. 2000. Potent competitive interactions of some brominated flame retardants and related compounds with human transthyretin in vitro. Toxicol Sci 56(1): 95-104.

Ness-Abramof R, Apovian CM. 2005. Drug-induced weight gain. Timely topics in medicine Cardiovascular diseases 9: E31.

Nolte RT, Wisely GB, Westin S, Cobb JE, Lambert MH, Kurokawa R, et al. 1998. Ligand binding and co-activator assembly of the peroxisome proliferator-activated receptor-gamma. Nature 395(6698): 137-143.

Noyes PD, Hinton DE, Stapleton HM. 2011. Accumulation and debromination of decabromodiphenyl ether (BDE-209) in juvenile fathead minnows (Pimephales promelas) induces thyroid disruption and liver alterations. Toxicol Sci 122(2): 265-274.

Ogden CL, Carroll MD, Kit BK, Flegal KM. 2012. Prevalence of obesity and trends in body mass index among US children and adolescents, 1999-2010. Jama 307(5): 483-490.

Patisaul HB, Roberts SC, Mabrey N, McCaffrey KA, Gear RB, Braun J, et al. 2013. Accumulation and endocrine disrupting effects of the flame retardant mixture Firemaster(R) 550 in rats: an exploratory assessment. J Biochem Mol Toxicol 27(2): 124-136.

Pillai HK, Fang M, Beglov D, Kozakov D, Vajda S, Stapleton HM, et al. 2014. Ligand Binding and Activation of PPARgamma by Firemaster(R) 550: Effects on Adipogenesis and Osteogenesis. Environ Health Perspect.

Qiu X, Mercado-Feliciano M, Bigsby RM, Hites RA. 2007. Measurement of polybrominated diphenyl ethers and metabolites in mouse plasma after exposure to a commercial pentabromodiphenyl ether mixture. Environ Health Perspect 115(7): 1052-1058.

Riu A, Grimaldi M, le Maire A, Bey G, Phillips K, Boulahtouf A, et al. 2011. Peroxisome Proliferator-Activated Receptor gamma Is a Target for Halogenated Analogs of Bisphenol A. Environ Health Persp 119(9): 1227-1232.

Roberts SC, Macaulay LJ, Stapleton HM. 2012. In vitro metabolism of the brominated flame retardants 2-ethylhexyl-2,3,4,5-tetrabromobenzoate (TBB) and bis(2-ethylhexyl) 2,3,4,5-tetrabromophthalate (TBPH) in human and rat tissues. Chem Res Toxicol 25(7): 1435-1441.

Rossi AM, Taylor CW. 2011. Analysis of protein-ligand interactions by fluorescence polarization. Nat Protoc 6(3).

Rudel RA, Camann DE, Spengler JD, Korn LR, Brody JG. 2003. Phthalates, alkylphenols, pesticides, polybrominated diphenyl ethers, and other endocrine-disrupting compounds in indoor air and dust. Environ Sci Technol 37(20): 4543-4553.

Springer C, Dere E, Hall SJ, McDonnell EV, Roberts SC, Butt CM, et al. 2012. Rodent Thyroid, Liver, and Fetal Testis Toxicity of the Monoester Metabolite of Bis-(2-ethylhexyl) Tetrabromophthalate (TBPH), a Novel Brominated Flame Retardant Present in Indoor Dust. Environ Health Persp 120(12): 1711-1719.

Stapleton HM, Eagle S, Sjodin A, Webster TF. 2012. Serum PBDEs in a North Carolina toddler cohort: associations with handwipes, house dust, and socioeconomic variables. Environ Health Perspect 120(7): 1049-1054.

Stapleton HM, Misenheimer J, Hoffman K, Webster TF. 2014. Flame retardant associations between children's handwipes and house dust. Chemosphere 30(14): 00039-00033.

Suzuki G, Tue NM, Malarvannan G, Sudaryanto A, Takahashi S, Tanabe S, et al. 2013. Similarities in the endocrine-disrupting potencies of indoor dust and flame retardants by using human osteosarcoma (U2OS) cell-based reporter gene assays. Environ Sci Technol 47(6): 2898-2908.

Tang-Peronard JL, Andersen HR, Jensen TK, Heitmann BL. 2011. Endocrine-disrupting chemicals and obesity development in humans: A review. Obes Rev 12(8): 622-636.

U.S. EPA. (2009) Child-specific exposure factors handbook. Available: http://cfpub.epa.gov/ncea/cfm/recordisplay.cfm?deid=55145. Accessed 2012 December 17.

Van den Eede N, Dirtu AC, Neels H, Covaci A. 2011. Analytical developments and preliminary assessment of human exposure to organophosphate flame retardants from indoor dust. Environ Int 37(2): 454-461.

Wang H, Zhou Y, Tang C, He Y, Wu J, Chen Y, et al. 2013. Urinary phthalate metabolites are associated with body mass index and waist circumference in Chinese school children. PloS one 8(2): e56800.

Watkins DJ, McClean MD, Fraser AJ, Weinberg J, Stapleton HM, Webster TF. 2013. Associations between PBDEs in office air, dust, and surface wipes. Environ Int 59: 124-132.

Table 1. IC_{50} values, dissociation constants (K_d), and the relative potency by setting rosiglitazone as 1.

Parent compounds* and metabolites	IC_{50} (μM)	K_d (μM)	Relative potency
Rosiglitazone	0.23	0.12	1.0000
TBB	NA	NA	NA
TBBA	42.0	22.10	0.0055
TBPH	NA	NA	NA
TBMEHP	0.64	0.34	0.3594
DEHP	NA	NA	NA
MEHP	3.80	2.00	0.0605
TPP	40.0	20.87	0.0058
DPP	627	327.13	0.0004
ITP	60.0	31.30	0.0038
TPT	1.72	0.90	0.1337
TPPi	>1,250	>652.17	<0.002
TBT	0.30	0.16	0.7667
TBuP	137	71.48	0.0017
TBEP	103	53.74	0.0022
BPA	NA	NA	NA
TCBPA	5.18	2.70	0.0444
TBBPA	1.49	0.78	0.1544
2,4,6–TFP	NA	NA	NA
2,4,6–TCP	100	52.17	0.0023
2,4,6–TBP	36.3	18.94	0.0063
2,4,6–TIP	1.84	0.96	0.1250
BDE–47	>12	>6.25	<0.16
3–OH BDE47	0.24	0.13	0.9583
5–OH BDE47	3.09	1.61	0.0744
6–OH BDE47	>10.0	>5.22	<0.023
BDE–99	NA	NA	NA
5'–OH BDE99	30.0	15.65	0.0077
6'–OH BDE99	>50	>26.09	<0.0046
Triclosan	12.5	6.52	0.0184

NA–No effect at 250 μM.

*The chemicals in bold represent the parent compounds.

Figure Legends

Figure 1. FP value (mP) of 1.25 nM PPAR–Green as a function of a) added TPP, and several FM550 metabolites including DPP, TBBA and TBMEHP and b) added 2,4,6–TFP, TCP, TBP and TIP concentration in 40 μL of 38 nM PPARγ LBD. Values represent the average of the triplicates, and error bars represent standard deviation.

Figure 2. FP value (mP) of 24 dust samples with a concentration of 3 mg dust/mL relative to the procedure dust blank in 40μL of 38 nM PPARγ LBD and 1.25 nM PPAR–Green. "1" represents DMSO control. "2" represents procedure blank. "3" represents the positive control of 12.5μM rosiglitazone. "4" represents SRM2585 and "6" is the DS6 used for dose–response. "5" and "7–12" represents the dust extracts which were used in the bioactivation. Values represent average of the triplicates and error bar represents standard deviation.

Figure 3. Competitive PPAR γ binding potency of rat liver S9 control, DEHP, Mixture (M.), SRM 2585 and other 7 dust samples (100 mg) by incubation with S9 and inactive S9 fraction with a concentration of 1mg protein/mL in a final volume of 3 mL. All data were normalized with the mP of S9 control. "M." includes 5μM FM550, ITP, BDE–47, BDE–99, and DEHP. SRM1 and SRM2 represent the incubation of SRM2585 with rat liver S9 and human liver S9, respectively. The dosing concentrations were 3mg DEQ/mL, 6 mg DEQ/mL, 2μM and 100μM for SRM2585, other dust samples, M., and DEHP; respectively. Values represent average of the triplicates and error bar represents standard deviation. Symbols without error bars represent one incubated sample.

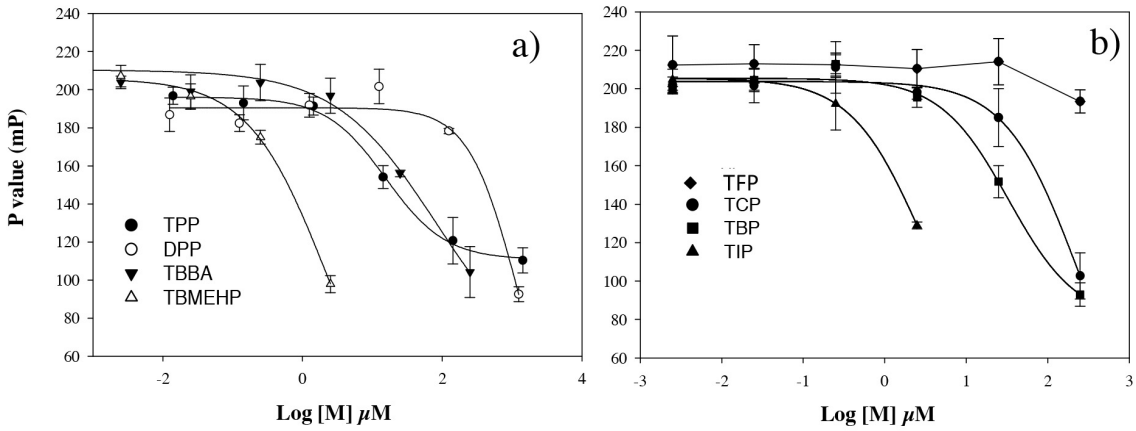
a)
b)
P value (mP)
Log [M] μM
Log [M] μM
TPP
DPP
TBBA
TBMEHP
TFP
TCP
TBP
TIP

Figure 1.

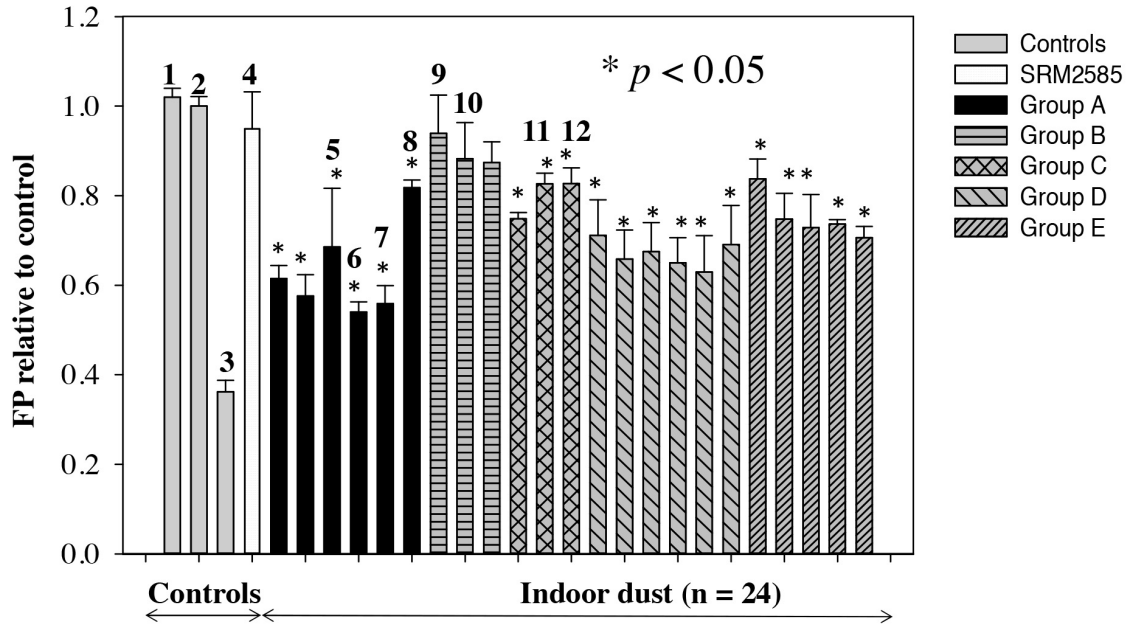
1.2
1.0
0.8
0.6
0.4
0.2
0.0
FP relative to control
* $p < 0.05$
1
2
3
4
5
6
7
8
9
10
11
12
Controls
Indoor dust (n = 24)
Controls
SRM2585
Group A
Group B
Group C
Group D
Group E

Figure 2.

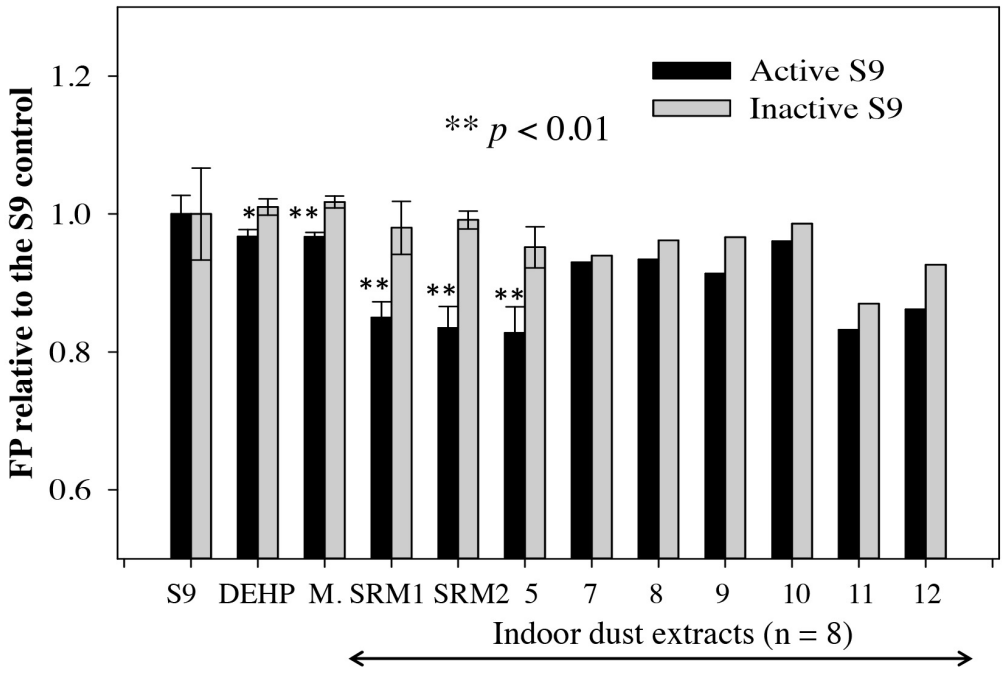
FP relative to the S9 control
1.2
1.0
0.8
0.6
Active S9
Inactive S9
** $p < 0.01$
S9
DEHP
M.
SRM1
SRM2
5
7
8
9
10
11
12
Indoor dust extracts (n = 8)

Figure 3.